Asian Journal of Social Science and Management Technology
ISSN: 2313-7410
Volume 7, Issue 4, July-August, 2025
Available at www.ajssmt.com

ANALYZING THE RELATIONSHIP BETWEEN LAND SURFACE TEMPERATURE AND THE SPATIAL PATTERN OF GREEN SPACE IN AKMEEMANA, BOPE-PODDALA AND GALLE FOUR GRAVETS DIVISIONAL SECRETARIAT DIVISIONS

K.W.K.A Priyadarshana[1], H.M.K.C.W Herath[2]

Department of Geography and Environmental Management, Sabaragamuwa University of Sri Lanka, Belihuloya, 70140

ABSTRACT:
The ongoing transformations in the spatial configurations of green spaces have emerged as a critical environmental issue of global significance, exerting profound impacts on both climatic dynamics and environmental quality. This study meticulously examines the spatiotemporal variations in green space patterns and their consequential influence on land surface temperature (LST) over a 24-year period, spanning from 2000 to 2024. The focal geographical scope encompasses the Akmeemana, Bope-Poddala, and Galle Four Gravets Divisional Secretariat Divisions in the Galle District, regions characterized by significant land use modifications attributable to historical, geographical, and socio-economic determinants. For this analysis, advanced Remote Sensing (RS) and Geographic Information Systems (GIS) technologies were employed, utilizing satellite imagery from Landsat 5TM, Landsat 8 OLI-TIRS, and Landsat 9 OLI-TIRS, acquired via the USGS Earth Explorer portal. These datasets facilitated the computation of the NDBI, NDVI, and LST for the selected years of 2000, 2008, 2016, and 2024. The linear regression analytical framework was utilized to elucidate the interrelationships among the variables. Results indicate a substantial decline in qualitative vegetation cover, from 77.48% of the land area in 2000 to 58.15% in 2024. Conversely, built-up land areas expanded significantly, from 8.72% in 2000 to 23.61% in 2024. This inverse relationship between vegetation cover and urban expansion correlates with an observable increase in land surface temperature over the studied period. The findings reveal that the mean LST value escalated by 1.63°C, from 25.91°C in 2000 to 27.54°C in 2024. Similarly, both the minimum and maximum LST values exhibited an upward trend, rising from 23.25°C to 24.72°C and from 25.91°C to 27.54°C, respectively. Noteworthy negative correlations between LST and NDVI, positive correlations between LST and NDBI, and negative correlations between NDVI and NDBI were identified. The investigation's findings underpin urban planning, environmental preservation, and sustainable land management. These insights are crucial for crafting policies to counter urbanization's climate and environmental impacts.

Keyword: GIS, LST, NDBI, NDVI, RS

---

1. Introduction

In today's rapidly urbanizing world, the spatial distribution of green spaces plays a vital role in influencing local climate and land surface temperatures. As urban areas continue to expand, the significance of green infrastructure becomes increasingly important. Therefore, it is essential to understand how variations in the distribution, size, and composition of green spaces impact land surface temperatures.(Estoque et al., 2017) . Urbanization, the fragmentation of green spaces, and changes in their spatial patterns due to various development activities have significantly influenced local microclimates and land surface temperatures. These changes have, in turn, affected both human well-being and ecological balance in multiple ways (Halefom et al., 2024) . Especially due to the concentration of high infrastructure facilities such as administration, education, capital, transportation, etc. in urban areas, a significant change in land use and land cover (LULC) can be identified in these areas. Accordingly, population growth and the corresponding wide spread of human needs have led to a clear change in human land use (Meyer & Turner, 1992). Rapid urbanization driven by population growth and the increasing appeal of urban living is projected to result in 68% of the global population residing in urban areas by 2050 (Nations, n.d.). This trend is expected to cause a significant reduction in green spaces due to changes in land use

According to the Food and Agriculture Organization's (FAO) Global Forest Resources Assessment 2020, forests covered approximately 4.06 billion hectares, accounting for about 31% of the world's total land area as of 2020 (*State of the World's Forests 2020*, n.d.). However, according to the World Wildlife Fund (WWF), approximately 18.7 million acres (7.6 million hectares) of forest are lost each year due to various factors, as reported in 2017 (*Forests*, n.d.). That is, based on current data on the rate of vegetation degradation, it is estimated that approximately 2,400 trees are cut down every minute ("Deforestation," 2025). Sri Lanka has been identified as one of the world's 34 biodiversity hotspots, highlighting its rich diversity of endemic plant and animal species found nowhere else on Earth. However, it is also noted that at least 70% of the natural habitats supporting these species have already been lost. Although it is generally recommended that a country maintain at least 35% forest cover, Sri Lanka currently has only about 20%. In the early 1800s, the island's forest cover stood at around 70%, but this has steadily declined, reaching just 29% by 2015. According to the Food and Agriculture Organization of the United Nations (FAO), since late 2005, Sri Lanka has ranked as the fourth country in the world in terms of annual loss of primary forest, with a deforestation rate of 1% per year (*ශ්‍රී ලංකාවේ වන විනාශය – Environment Foundation (Guarantee) Limited.*, n.d.).

Accordingly, increasing demand and competition for land a limited and valuable resource have led to growing pressure on existing vegetation cover, which serves as the natural layer of the land. As a result, the conversion of natural landscapes into built-up areas for various human purposes, including residential, agricultural, economic, and infrastructure development, has accelerated (*Study Session 5 Urbanisation: Trends, Causes and Effects: View as Single Page | OLCreate*, n.d.).

Large subnational region			Total			
Small subnational region			Total			
Variable			Area built-up before			
Year			1975	1990	2000	2014
Country	**Measure**	**Unit**				
World	Square kilometers	Square kilometers	377,463.57	520,573.23	652,203.34	784,840.93
	Percent of total land area	Percentage	0.29	0.40	0.50	0.60
Sri Lanka	Square kilometers	Square kilometers	511.11	654.42	773.57	906.07
	Percent of total land area	Percentage	0.78	0.99	1.18	1.38
Data extracted on 25 Apr 2024 16:15 UTC (GMT) from OECD.Stat						

Table 01: Growth of Global and Sri Lankan Built-up Areas (1975–2014)

According to the latest data updated in 2020 by the Organization for Economic Co-operation and Development (OECD), as shown in Table 1, the world's built-up area nearly doubled between 1975 and 2014. This highlights the significant and ongoing transformation of human land use on a global scale. This trend is evident not only worldwide but also in Sri Lanka. This can be clearly understood by referring to Table 1. For instance, according to data from the Ministry of Transport and Highways, Sri Lanka's road network expanded from 12,000 kilometers in 2005 to 14,000 kilometers in 2020. Similarly, the Department of Census and Statistics reports that the number of housing units in the country increased from 4.3 million in 2001 to 5.2 million in 2012 (*CPH_2012_5Per_Rpt.Pdf*, n.d.).

Accordingly, an increase in the Earth's surface temperature can currently be observed as a result of expanding built-up areas and the gradual loss of vegetation cover (Rendana et al., 2023). Temperature is a highly sensitive factor that plays a critical role in sustaining life on Earth. Even minor changes in temperature can lead to complex environmental and human-related challenges (Rocha et al., 2022). In recent years, it has become possible to observe temperature changes on the Earth's surface that go beyond natural fluctuations (*Earth's Changing Climate*, n.d.). These are commonly reflected as variations in global temperature. According to an ongoing temperature analysis conducted by scientists at NASA's Goddard Institute for Space Studies (GISS), the average global temperature on Earth has increased by at least 1.1°C (1.9°F) since 1880. Most of this warming has occurred since 1975, with temperatures rising at a rate of approximately 0.15 to 0.20°C per decade. (*World of Change*, 2020).

These global temperature trends can also be observed in Sri Lanka. Although spatial and temporal variations in temperature exist due to the country's diverse geological and climatic conditions, average temperature levels across all regions have shown noticeable changes compared to the past (Meegahakotuwa & Nianthi, 2023) . Accordingly, these changes can be examined using the capabilities of modern technology. By analyzing the absorption and reflection characteristics of electromagnetic waves from various surface features through advanced methods such as remote sensing and geographic information system (GIS) technologies and by interpreting satellite data collected from space, it is possible to study both the spatial and temporal changes in green spaces and the resulting variations in land surface temperature (*Remote Sensing | NASA Earthdata*, n.d.). Accordingly, this research focuses on examining the relationship between changes in the spatial pattern of green spaces and land surface temperature. It aims to address existing gaps in the research literature on this topic. Specifically, the study investigates changes in green space and the resulting variations in land surface temperature as a key environmental issue within the Galle Four Gravets, Akmeemana, and Bope-Poddala Divisional Secretariat Divisions during the period from 2000 to 2024.

2. Material and Methods

Study Area

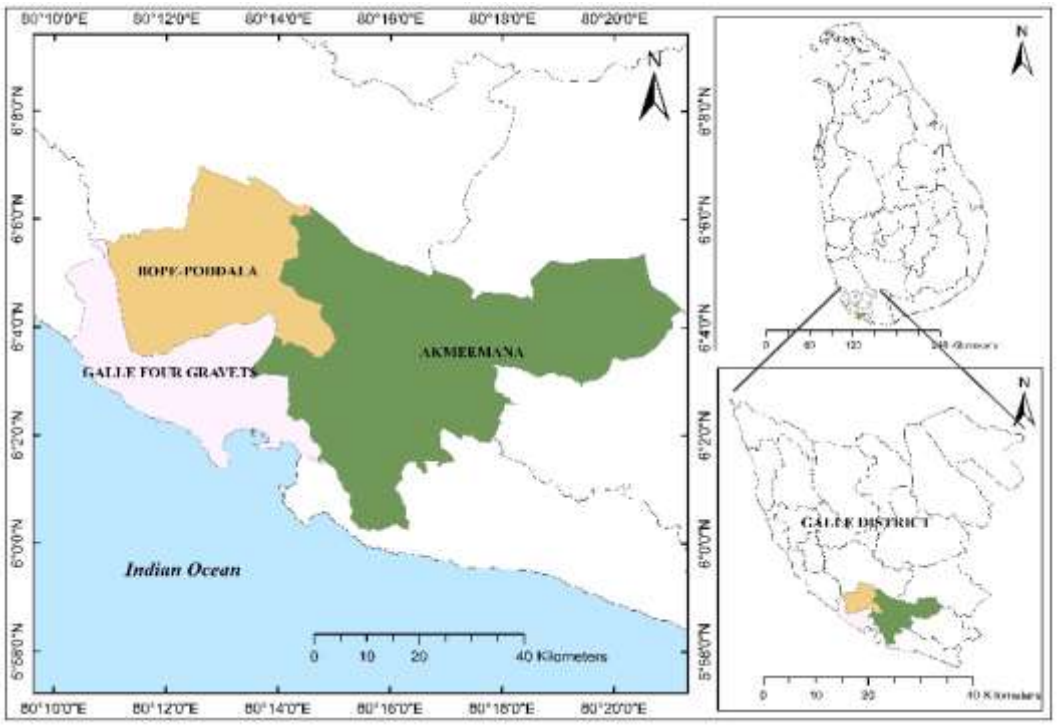

Fig.1.Study Area Map

The study area includes the three Divisional Secretariat Divisions of Akmeemana, Bope-Poddala, and Galle Four Gravets, located in the Galle District of Sri Lanka's Southern Province. Geographically, the area lies between 80°10' and 80°21' East longitude and between 6°00' and 6°07' North latitude. The total extent of the study area is approximately 119.66 square kilometers (11,966 hectares), accounting for about 7.5% of the total land area of the Galle District (*2016.Pdf*, n.d.).

This region falls within the South-West Coastal Low Plains and lies entirely within the 500-foot contour above sea level. It receives an average annual rainfall of 2,307 mm, while the average annual temperature is from 24℃ - 33℃ (*Overview*, n.d.).

In terms of demographic and social background, the area is home to a population of 268,386 individuals from various ethnic backgrounds. Of this population, 139,992 (52.16%) are female and 128,394 (47.83%) are male (*1686217885054609.Pdf*, n.d.). The region has a high population density and a predominantly urban population. Since many of the administrative functions and development activities of the Galle District are concentrated in this area, it is undergoing rapid urbanization. Consequently, built-up areas are expanding rapidly, posing a significant threat to the remaining natural green spaces.

Data Collection

To achieve the objectives of this research, both quantitative and qualitative research methods were applied. The study is primarily based on secondary data, with satellite image analysis used as the main tool for primary analysis. Landsat 5 TM, Landsat 8 OLI-TIRS, and Landsat 9 OLI-TIRS satellite images corresponding to the study period were obtained from the United States Geological Survey (USGS) website. Detailed information about these satellite images is presented in Table 02.

The spatial resolution of the satellite imagery ranges from 30 to 120 meters. To ensure data quality and reliability, satellite images were selected with cloud cover limited to 10% or less (≤10). Using four satellite images spaced at 8-year intervals between 2000 and 2024, the Normalized Difference Vegetation Index (NDVI),

Normalized Difference Built-Up Index (NDBI), and Land Surface Temperature (LST) Index were calculated to assess spatial and temporal changes in green space and land surface temperature

Year	Satellite Sensor	Path	Row	Wave Band		Spectral Range(µm)		Spatial Resolution	Cloud Cover
				NIR	RED	NIR	RED		
2000	Landsat 5 TM	141	056	4	3	0.76-0.90	0.63-0.69	30m	≤10%
2008	Landsat 5 TM	141	056	4	3	0.76-0.90	0.63-0.69	30m	≤10%
2016	Landsat 8 OLI-TIRS	141	056	5	4	0.845-0.885	0.63-0.68	30m	≤10%
2024	Landsat 9 OLI-TIRS	141	056	5	4	0.845-0.885	0.63-0.68	30m	≤10%

Table 02: Information about the data obtained for the research

Data	Resolution	Source	Year
Landsat 5TM	Multispectral: 30 m; Thermal:120 m	USGS Earth Explorer (https://earthexplorer.usgs.gov/)	2000, 2008, 2016, 2024
Landsat 8 OLI-TIRS	Multispectral: 30 m; Thermal:100 m		
Landsat 9 OLI-TIRS			
Digital Layers	1:50,000	Sri Lanka Survey Department	

Analysis Techniques

The data analysis in this study, which investigates the relationship between land surface temperature and the spatial variation of green space, is conducted using two main approaches, remote sensing analysis techniques and statistical analysis. Under the remote sensing approach, three key indices are calculated Normalized Difference Vegetation Index (NDVI), Land Surface Temperature (LST), and Normalized Difference Built-up Index (NDBI). For the statistical analysis, linear regression analysis is used to examine the relationships between these variables.

Normalized Difference Vegetation Index (NDVI)

$$NDVI = \frac{(NIR - RED)}{(NIR + RED)}$$

The Normalized Difference Vegetation Index (NDVI) is a widely used indicator for assessing vegetation presence, density, and health on the Earth's surface (*Landsat Normalized Difference Vegetation Index | U.S. Geological Survey*, n.d.). It serves as an effective tool to distinguish vegetated areas from non-vegetated surfaces such as bare land or built-up areas. Green vegetation absorbs a significant portion of red light while reflecting a substantial amount of near-infrared (NIR) radiation. This is because the chlorophyll pigment in plant leaves strongly absorbs visible light (400–700 nm) for photosynthesis, while the internal cellular structure of leaves reflects NIR radiation (700–1100 nm) (*What Is Normalized Difference Vegetation Index (NDVI)?*, 2025). Accordingly, the details of the satellite images used to calculate the Normalized Difference Vegetation Index (NDVI) are given in Table 03 below.

Table 03: Information on Satellite Imagery Used for NDVI Calculation

Normalized Difference Built-up Index (NDBI).

$$NDBI = \frac{(SWIR - NIR)}{(SWIR + NIR)}$$

The Normalized Difference Built-up Index (NDBI) is a remote sensing-derived spectral index designed to detect and quantify built-up or urbanized areas within a landscape (Zha et al., 2003). It serves as an effective tool for evaluating the spatial extent, distribution, and density of human-made structures such as buildings, roads, and

other impervious surfaces. NDBI utilizes reflectance values from the Near-Infrared (NIR) and Shortwave Infrared (SWIR) bands of the electromagnetic spectrum, typically obtained from satellite sensors such as Landsat (*NDBI—ArcGIS Pro | Documentation*, n.d.). In the electromagnetic spectrum, NIR wavelengths range approximately from 0.7 to 1.4 micrometers, while SWIR spans from 1.4 to 3 micrometers. In practical applications using Landsat imagery, NIR is usually centered around 0.76 – 0.90 µm, and SWIR around 1.55–1.75 µm. Healthy vegetation strongly reflects NIR radiation and absorbs SWIR, whereas built-up areas composed of materials like concrete and asphalt exhibit higher SWIR reflectance than NIR. This spectral contrast forms the basis of the NDBI. Accordingly, details of the satellite imagery used to calculate the NDBI are given in Table 04.

Table 04: Information on Satellite Imagery Used for NDBI Calculation

Year	Satellite Sensor	Path	Row	Wave Band	Spectral Range(µm)	Spatial Resolution	Cloud Cover
				Thermal	Thermal		
2000	Landsat 5 TM	141	056	Band 6	10.40 - 12.50	120 m	≤10%
2008	Landsat 5 TM	141	056	Band 6	10.40 - 12.50	120 m	≤10%
2016	Landsat 8 OLI-TIRS	141	056	Band 10 (TIRS 1)	10.6 - 11.19	100 m	≤10%
2023	Landsat 9 OLI-TIRS	141	056	Band 10 (TIRS 1)	10.6 - 11.19	100 m	≤10%

Land Surface Temperature (LST)

Land Surface Temperature (LST) refers to the amount of heat energy emitted or absorbed by the Earth's surface elements such as land, water, and ice. It is a key variable in environmental monitoring and can be accurately measured through satellite-based infrared sensing techniques (*Land Surface Temperature*, n.d.). In this study, LST was calculated for the years 2000, 2008, 2016, and 2024 using satellite imagery from Landsat 5 TM, Landsat 8 OLI-TIRS, and Landsat 9 OLI-TIRS. The details of the satellite images used for LST calculation are presented in Table 05.

Table 05: Information on Satellite Imagery Used for LST Calculation

Year	Satellite Sensor	Path	Row	Wave Band		Spectral Range(µm)		Spatial Resolution	Cloud Cover
				(SWIR) 1	NIR	(SWIR)1	NIR		
2000	Landsat 5 TM	141	056	5	4	1.55 - 1.75	0.76-0.90	30m	≤10%
2008	Landsat 5 TM	141	056	5	4	1.55 - 1.75	0.76-0.90	30m	≤10%
2016	Landsat 8 OLI-TIRS	141	056	6	5	1.57 - 1.65	0.85-0.88	30m	≤10%
2023	Landsat 9 OLI-TIRS	141	056	6	5	1.57 - 1.65	0.85-0.88	30m	≤10%

Accordingly, there are several key steps to follow when calculating the Land Surface Temperature (LST) index using this data. These steps include,

1. Conversion of Digital Numbers (DN) to spectral /Top of Atmosphere (TOA) Radiance (Lλ)

In this phase, radiometric corrections were performed on the Landsat 5, Landsat 8, and Landsat 9 satellite imagery used as research data. The purpose of performing radiometric corrections is to correct and minimize errors caused by sunlight, weather conditions, atmospheric disturbances, and other factors in recording satellite imagery data, so that the resulting information becomes more accurate and reliable. That is, this transformation ensures that the radiation values represent the actual energy measured by the sensor, allowing for consistent comparison across different time periods and sensors (*RS Ch 4 RS Preprocessing.Pdf*, n.d.).

It is important to note that the procedure for estimating Land Surface Temperature (LST) from Landsat 5 Thematic Mapper (TM) imagery differs slightly from the procedure used for Landsat 8 and Landsat 9 Operational

Land Imager–Thermal Infrared Sensor (OLI-TIRS) imagery. These differences arise due to the sensor specifications, thermal bands used, and calibration constants specific to each satellite. Therefore, the radiometric calibration, conversion to brightness temperature, and the estimation of surface emissivity are carried out in accordance with the respective algorithms and parameters suitable for each Landsat generation. The Digital Number (DN) values of the thermal band were used to calculate the Spectral Radiance (Lλ) for Landsat 5, as given in Equation 01. In contrast, for Landsat 8 and Landsat 9, the Top of Atmosphere (TOA) spectral radiance was calculated using Equation 02, which incorporates sensor-specific radiometric rescaling factor

Equation 01 – Spectral Radiance for Landsat 5 TM

$$L_\lambda = \left(\frac{LMAX_\lambda - LMIN_\lambda}{Q_{cal\,max} - Q_{cal\,min}}\right)(Q_{cal} - Q_{cal\,\min}) + LMIN_\lambda$$

Q_{cal} = the image value (DN)
$Q_{cal\,min}$ = Minimum quantized calibrated pixel value corresponding to $LMIN_\lambda$(1)
$Q_{cal\,max}$ = Maximum quantized calibrated pixel value corresponding to $LMAX_\lambda$ (255)
$LMIN_\lambda$ = Spectral– at sensor radiance that is scaled to $Q_{cal\,min}$[W/(m^2 sr µm)] (1.238)
$LMAX_\lambda$ = Spectral – at sensor radiance that is scaled to $Q_{cal\,max}$[W/(m^2 sr µm)] (15.303)

Equation 02 – Top of Atmosphere (TOA) Spectral Radiance for Landsat 8/9 OLI-TIRS

$$L_\lambda = M_L \times Q_{cal} + A_L$$

L_λ = TOA spectral radiance
M_L = Band specific multiplicative rescaling factor (0.0003342)
A_L = Band specific additive rescaling factor (0.10000)
Q_{cal} = Quantized and Calibrated standard Product Pixel Value (DN)

2. Conversion of DN to At-Satellite Brightness Temperature

Once the spectral radiance is obtained from the thermal band of the satellite image, it is then converted into brightness temperature (BT) the temperature of a blackbody that would emit the same radiance at a given wavelength. This conversion is performed using the calibration constants specific to each Landsat sensor, and the results are in Kelvin (K). These Kelvin values are subsequently converted to degrees Celsius (°C) for easier interpretation in climatological studies. The formula for converting spectral radiance to brightness temperature is as follows

Equation 03

$$BT = \frac{K_2}{\ln(\frac{K_1}{L_\lambda}+1)} - 273.15$$

K_1, K_2 = the calibration constants.
BT = brightness temperature [°C]
L_λ = the spectral radiation

Parameters	Landsat 5	Landsat 8/9
K_1	607.76	774.89
K_2	1260.56	1321.08

3. Calculation of Land Surface Emissivity (LSE)

Land Surface Emissivity (LSE) is a crucial parameter in accurately estimating Land Surface Temperature (LST), as it represents the efficiency with which a surface emits thermal radiation. Since different surface materials (e.g., vegetation, soil, and urban structures) emit varying amounts of thermal energy, emissivity must be carefully considered to avoid significant errors in LST estimation. Emissivity is particularly influenced by the fractional vegetation cover of the surface, which can be quantified using the Normalized Difference Vegetation Index

(NDVI). Based on NDVI values, the proportion of vegetation (PV) is derived, which in turn is used to calculate the emissivity (LSE) for each pixel.

Equation 04 – Normalized Difference Vegetation Index (NDVI)

$$NDVI = \frac{(NIR - RED)}{(NIR + RED)}$$

Equation 05 – Proportion of Vegetation (PV)

$$PV = (\frac{\text{NDVI} - NDVI_{min}}{NDVI_{max} - NDVI_{min}})^2$$

NDVI	=	DN Values from NDVI Image
$NDVI_{min}$	=	Minimum DN Values from NDVI Image
$NDVI_{max}$	=	Maximum DN Values from NDVI Image

Equation 06 – Land Surface Emissivity (LSE)

$$\text{LSE} = 0.004 \times PV + 0.986$$

4. Calculation of Land Surface Temperature (LST)

After completing the previous steps, the final Land Surface Temperature (LST) was obtained using the following Equation (07).

Equation 07

$$LST = \frac{\text{BT}}{1 + (\frac{\lambda \times BT}{\text{P}}) \times \ln(LSE)}$$

BT - Top of atmosphere brightness temperature
LSE - the spectral emissivity
λ - the wavelength of the emitted radiance
h - Planck's constant (h = $6.626*10^{-34}$Js
s - Boltzmann's constant (s = $1.38*10^{-23} J/K$)
c - velocity of light (c = $2.998 * 10^8$ m/s)
P = h*c/s = $1.4388*10^{-2}$mk

3. Results

Analysis of Vegetation Cover Changes Based on NDVI Results (2000–2024)

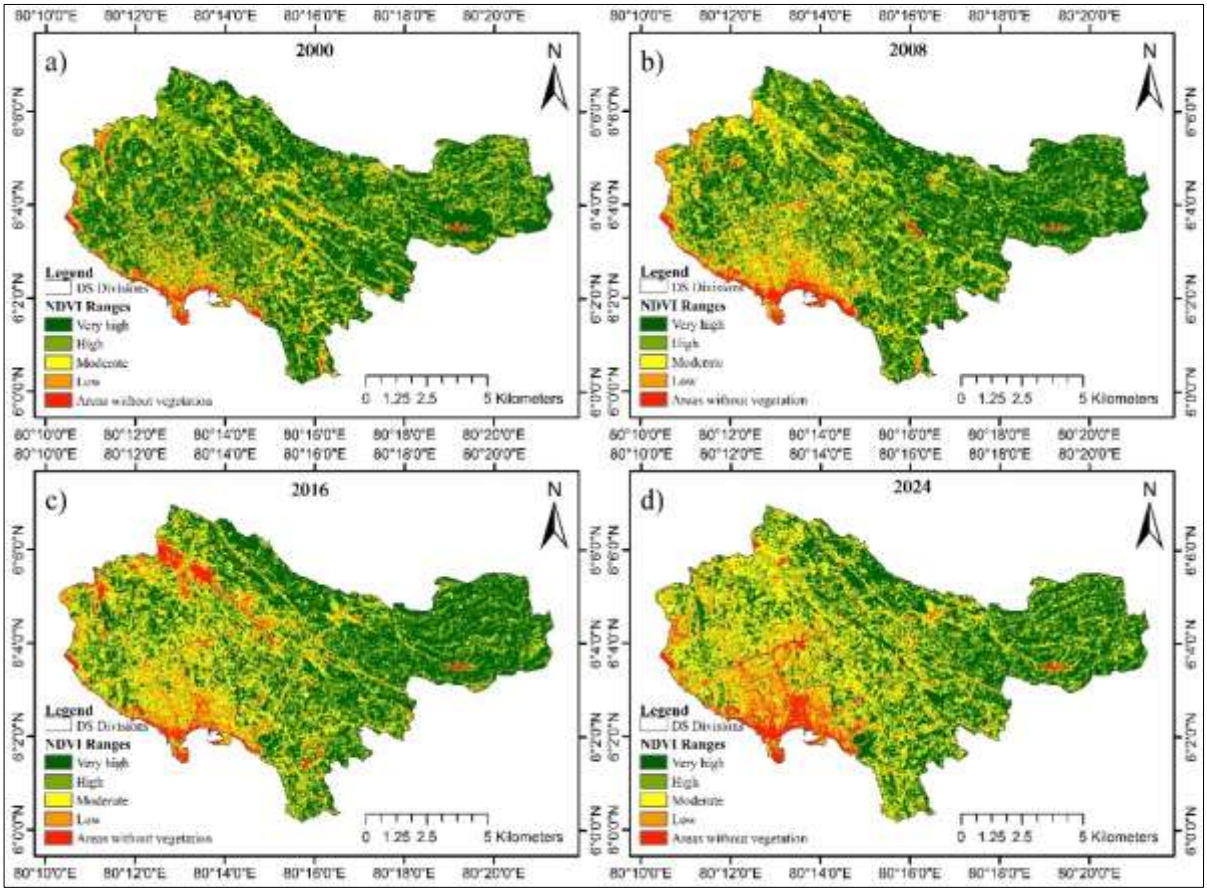

Fig.2: Normalized difference vegetation index (NDVI), 2000(a), 2008(b), 2016(c), 2024(d)

To examine the spatial and temporal variations in vegetation cover within the study area, a generalized vegetation index was calculated using remote sensing and Geographic Information System (GIS) technologies. Vegetation cover changes over a 24-year period were analyzed using satellite imagery obtained at eight-year intervals—namely, for the years 2000, 2008, 2016, and 2024 (Fig. 2). According to the results, a consistent decrease in vegetation cover across the study area can be observed from 2000 to 2024.

Table 06: Area of land belonging to each NDVI category

NDVI classification	Years							
	2000		2008		2016		2024	
	Land area (km^2)	Percentage (%)	Land area (km^2)	Percentage (%)	Land area (km^2)	Percentage (%)	Land area (km^2)	Percentage (%)
Non Vegetation	2.25	1.84	3.43	2.81	4.50	3.68	6.03	4.93
Low	9.01	7.38	9.05	7.41	12.66	10.37	13.06	10.69
Moderate	16.32	13.36	20.52	16.81	25.43	20.83	31.99	26.2
High	41.56	34.04	39.88	32.67	34.54	28.3	33.59	27.51
Very high	52.93	43.36	49.19	40.29	44.93	36.8	37.40	30.64

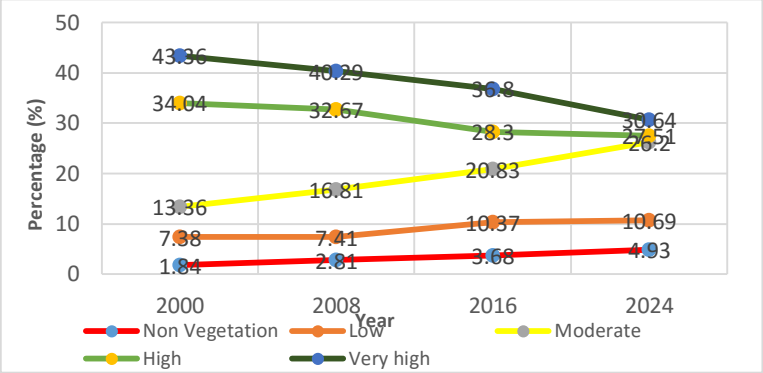

Fig.3: Temporal change in vegetation cover, 2000-2024

As detailed in Table 06, in the year 2000, out of the total 122.06 km² land area spanning the four Divisional Secretariat Divisions Akmeemana, Bope Poddala, and Galle Four Gravets a very high vegetation cover was observed over 52.93 km², which accounted for 43.36% of the total area. Additionally, 41.56 km² of the land area fell under the category of high vegetation cover. Thus, the total extent of quality vegetation cover (very high + high) in 2000 was 94.49 km², indicating a relatively healthy vegetation status.

In contrast, moderate vegetation cover accounted for 16.32 km², while areas with very low vegetation cover and no vegetation cover were 9.01 km² and 2.25 km², respectively. Therefore, the combined area with minimal or no vegetation was 11.26 km², representing 9.22% of the total land area.

A comparative assessment of data for the year 2008 reveals notable changes. The area with very high vegetation cover decreased to 49.19 km², and high vegetation cover declined to 39.88 km². Accordingly, the extent of quality vegetation cover dropped to 81.86 km² a decrease of 5.42 km² compared to 2000. Meanwhile, the area with moderate vegetation cover increased to 20.52 km², and areas with very low and no vegetation cover rose to 9.05 km² and 3.43 km², respectively. Thus, a total of 12.48 km² was identified as having minimal or no vegetation cover an increase of 1.22 km² compared to the year 2000. These findings indicate an emerging trend of vegetation loss across the landscape.

By 2016, the results derived from NDVI analysis indicate a further decline. The area under very high vegetation cover decreased to 44.93 km², while high vegetation cover dropped to 34.54 km². Thus, the quality vegetation cover stood at 79.47 km². Meanwhile, moderate vegetation cover increased to 25.43 km². The area with very low vegetation cover expanded to 12.66 km², and areas with no vegetation cover increased to 4.50 km². Altogether, the total extent of land with minimal or no vegetation cover reached 17.16 km².

Focusing on the temporal progression from 2000 to 2024, the NDVI-based analysis reveals a significant decline in high vegetation coverage. In 2000, areas with very high vegetation cover accounted for 43.36% of the total land area. This figure declined to 40.29% in 2008 and further dropped to 36.8% in 2016 an overall decrease of 9.72 percentage points from 2000. Likewise, the extent of land with high vegetation cover dropped from 34.04% in 2000 to 27.51% by 2024.

The trend of vegetation degradation is further underscored by the increase in areas with very low and no vegetation cover. While only 7.38% of the study area had minimal vegetation in 2000, this increased to 10.69% by 2024. Similarly, areas devoid of vegetation grew from 1.84% in 2000 to 2.81% in 2008, 3.68% in 2016, and reached 4.93% by 2024 more than doubling over the 24-year period.

In summary, the results of the NDVI analysis clearly demonstrate a gradual but consistent spatial and temporal degradation of vegetation cover in the Akmeemana, Bope Poddala, and Galle Four Gravets Divisional Secretariat Divisions between 2000 and 2024.

Analysis of Changes in Built-up Areas Based on NDBI Results (2000–2024)

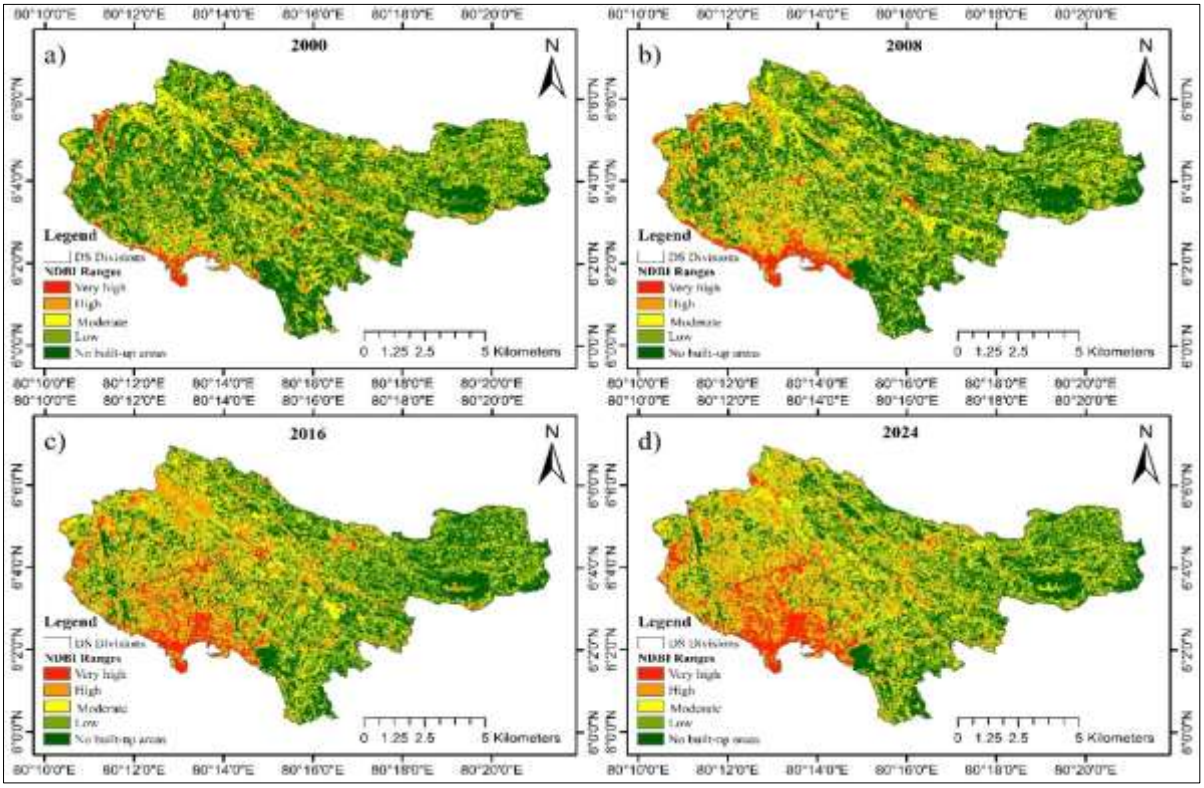

Fig.4: Normalized Difference Built-up Index (NDBI), 2000(a), 2008(b), 2016(c), 2024(d)

To examine spatial and temporal changes in built-up areas, the Normalized Difference Built-up Index (NDBI) was calculated using remote sensing and GIS for the years 2000, 2008, 2016, and 2024. The results show a steady increase in built-up areas over the 24-year period, indicating ongoing urban expansion across the study area (fig).

Table 06: Area of land belonging to each NDBI category

NDBI Classification	Years							
	2000		2008		2016		2023	
	Land area (km^2)	Percentage (%)	Land area (km^2)	Percentage (%)	Land area (km^2)	Percentage (%)	Land area (km^2)	Percentage (%)
No built Up Area	39.03	31.97	36.53	29.93	30.02	24.59	25.61	20.98
Low	47.45	38.87	42.67	34.95	37.33	30.58	36.93	30.25
Moderate	24.93	20.42	28.40	23.26	28.45	23.31	30.69	25.14
High	6.84	5.6	9.65	7.9	18.96	15.53	20.19	16.53
Very High	3.81	3.12	4.81	3.93	7.30	5.97	8.65	7.08
NDBI Classification	Years							
	2000		2008		2016		2023	
	Land area (km^2)	Percentage (%)	Land area (km^2)	Percentage (%)	Land area (km^2)	Percentage (%)	Land area (km^2)	Percentage (%)
No built Up Area	39.03	31.97	36.53	29.93	30.02	24.59	25.61	20.98
Low	47.45	38.87	42.67	34.95	37.33	30.58	36.93	30.25
Moderate	24.93	20.42	28.40	23.26	28.45	23.31	30.69	25.14
High	6.84	5.6	9.65	7.9	18.96	15.53	20.19	16.53
Very High	3.81	3.12	4.81	3.93	7.30	5.97	8.65	7.08

Fig.5: Temporal change in built-up areas, 2000-2024

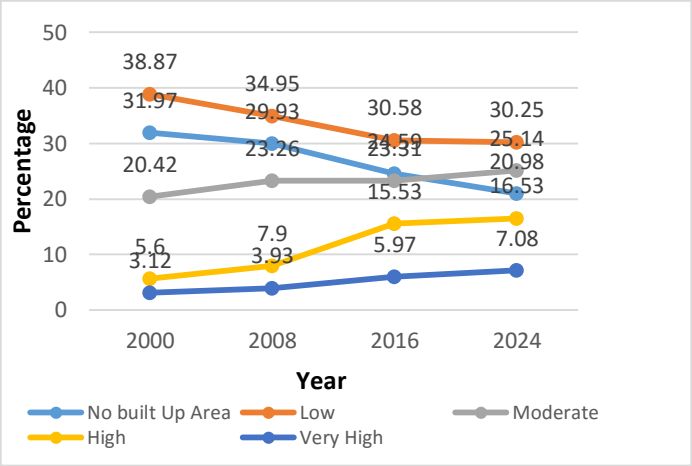

As detailed in Table 06, built-up areas were relatively limited in the year 2000. Very high built-up areas accounted for approximately 3.81 km², while high built-up areas covered around 6.84 km². Altogether, these accounted for 10.65 km², or about 8.72% of the study area. Moderately built-up areas extended over 24.93 km², whereas minimal and non-built-up areas were significantly larger, covering 47.45 km² and 39.03 km² respectively. These low-intensity or non-built-up areas collectively spanned 86.48 km² (over 70% of the total area), suggesting extensive vegetation or undeveloped land during this period.

By 2008, a measurable increase in built-up intensity was observed. Very high built-up areas increased to 4.80 km², and high built-up areas to 9.64 km², totaling 14.44 km². Moderate built-up areas also increased to 28.40 km², whereas minimal and non-built-up zones reduced to 42.66 km² and 36.53 km² respectively. This shift suggests a trend toward urban expansion and infrastructure development.

This trend continued in 2016. Very high built-up areas expanded to 7.29 km², and high built-up areas to 18.95 km². Together, these zones comprised 26.24 km². Meanwhile, moderate built-up areas slightly increased to 28.45 km². Areas with minimal and no built-up presence continued to decline, accounting for 37.33 km² and 30.01 km² respectively, indicating a further transition from vegetated or undeveloped land to more developed areas.

By 2024, the most significant change in built-up extent was recorded. Very high built-up areas reached 8.64 km² marking a 226.92% increase from the year 2000. High built-up areas covered 20.18 km², leading to a combined 28.82 km² (23.61% of the study area) classified as either highly or very highly developed. Moderate built-up zones also grew to 30.68 km². Simultaneously, areas with minimal and no built-up presence declined to 37.26 km² and 25.27 km², respectively. The collective extent of minimally and non-built-up land reduced from 86.46 km² in 2000 to 62.53 km² in 2024, a decline of 23.93 km².

In percentage terms, the study area experienced a steady rise in built-up land intensity. Very high built-up areas increased from 3.12% in 2000 to 7.08% by 2024. Similarly, highly developed areas rose from 5.6% to 16.53% of the total land area. Thus, areas with high and very high development expanded from 8.72% to 23.61% over the study period. Conversely, minimally built-up and non-built-up areas declined notably from 38.87% and 31.97% respectively in 2000 to 30.25% and 20.98% by 2024.

Land Surface Temperature (LST) Variation Analysis from 2000 to 2024

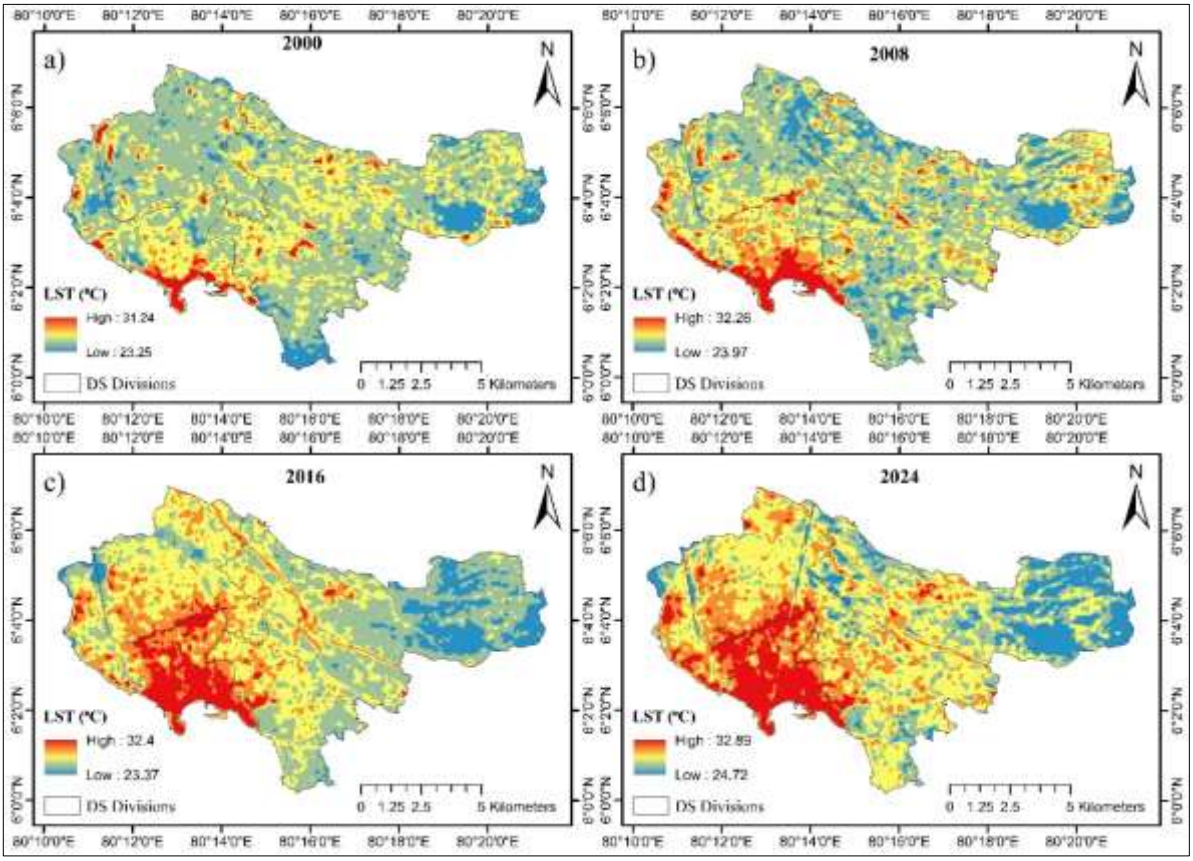

Fig.06: land surface temperature (LST), 2000(a), 2008(b), 2016(c), 2024(d)

The spatial and temporal distribution of land surface temperature (LST) for the years 2000, 2008, 2016, and 2024 across the Akmeemana, Bope-Poddala, and Galle Four Gravets Divisional Secretariat Divisions is clearly illustrated in Figure 06. The analysis reveals that LST is directly influenced by the patterns of urbanization and the spatial distribution of vegetation cover in the study area. Notably, areas with high LST are prominently concentrated in the urban and peri-urban zones surrounding Galle city, which already showed low vegetation cover and extensive built-up areas by the year 2000.

With the progressive expansion of urban infrastructure and the reduction of green cover, areas exhibiting high LST have spatially expanded. This expansion is particularly evident around Galle city, which, being a major coastal city in southern Sri Lanka, has experienced significant urban growth. Due to the coastal setting, this urban expansion has predominantly extended northward, and this pattern is mirrored in the spatial distribution of elevated land surface temperatures.

Table 07: Land surface temperature variation (2000-2024)

Year	Temperature (°C)		
	Minimum temperature	**Maximum temperature**	**Average temperature**
2000	23.25	31.24	25.91
2008	23.97	32.26	26.76
2016	23.37	32.4	26.91
2024	24.72	32.9	27.54

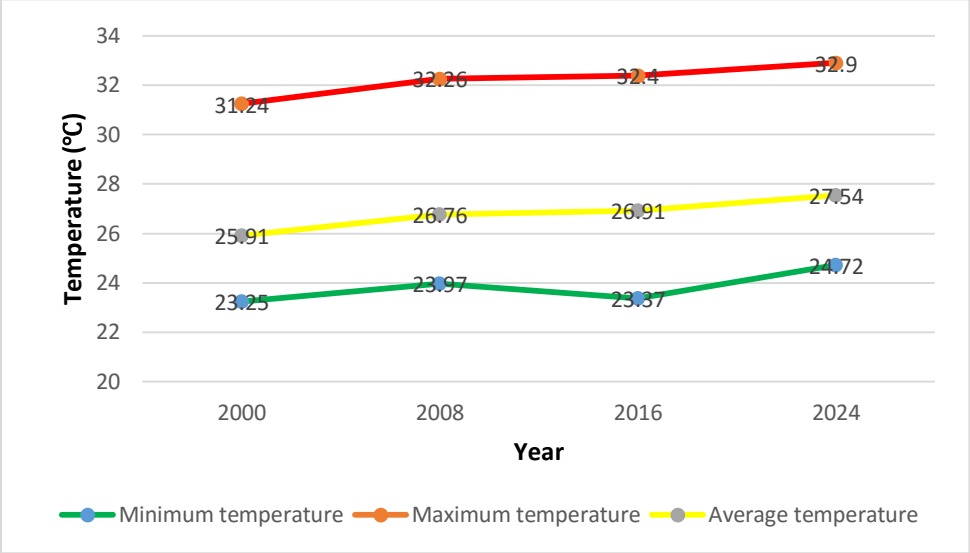

Fig.07: Temporal change in built-up areas (2000-2024)

Over the 24-year study period (2000–2024), significant variations in LST were observed within the three Divisional Secretariat Divisions. In 2000, the minimum recorded land surface temperature was 23.25°C, while the maximum reached 31.24°C. By 2008, both minimum and maximum temperature values showed a noticeable increase. The minimum temperature rose by 0.72°C to 23.97°C, and the maximum increased by 1.02°C to 32.26°C. In 2016, although the minimum LST experienced a slight decline compared to 2008, the maximum LST continued to rise, reaching 32.4°C, which marks an increase of 0.14°C from the previous maximum. By 2024, the highest LST values of the entire study period were recorded. The minimum LST rose to 24.72°C an increase of 1.35°C from 2016 while the maximum LST reached 32.9°C, which is 0.5°C higher than the maximum recorded in 2016.

Overall, from 2000 to 2024, the minimum LST in the study area increased by 1.47°C, and the maximum LST rose by 1.66°C. These trends indicate a consistent rise in surface temperatures across the region over the 24-year period. This increase is also reflected in the average LST values. In 2000, the average LST was recorded at 25.91°C. It rose to 26.76°C in 2008, 26.91°C in 2016, and reached its peak at 27.54°C in 2024. This represents a total increase of 1.63°C in the average LST over the study period.

4. Discussion

A key finding in the study of land surface temperature in the Divisional Secretariat Divisions of Akmeemana, Bope-Poddala, and Galle Four Gravets is that variations in built-up areas and vegetation cover have significantly contributed to the observed changes in land surface temperature. Over the years 2000, 2008, 2016, and 2024, a rapid decline in vegetation cover is evident throughout the study area. In the year 2000, areas with high and very high vegetation cover accounted for 77.40% of the total land area, while areas with high and very high built-up development comprised only about 8.72%. During this period, the average land surface temperature was recorded at 25.91°C. By 2008, vegetation cover had declined to 72.96%, while built-up areas had expanded to 11.83% of the total land area. Correspondingly, the average land surface temperature rose to 26.76°C. This pattern of decreasing vegetation and increasing urban development continued in 2016, where high and very high vegetation cover fell further to 65.10%, and built-up areas increased significantly to 21.5%. In 2024, vegetation cover dropped again to 58.15%, marking a 19.25% decrease compared to 2000, while high and very high built-up areas increased to 23.61% a rise of 14.88% from the year 2000. Alongside these land cover changes, the average land surface temperature also rose, reaching 27.54°C in 2024. These trends clearly indicate that the continuous loss of green space due to the expansion of built-up areas has directly contributed to rising land surface temperatures in the region.

This relationship is further supported by a study conducted by D.M.S.L.B. Dissanayake in 2019 on the impact of land use changes on land surface temperature within the Galle Municipal Council area. According to that study, between 1996 and 2019, built-up areas in the region increased by 38%, while vegetation cover and unbuilt-up areas decreased by 26% and 12%, respectively. During the same period, the average land surface temperature rose by 3.2°C (Dissanayake, 2020). The findings from both studies this one and Dissanayake's clearly confirm that rapid urbanization and green space degradation are key drivers of the gradual increase in land surface temperature in the study area.

This conclusion is visually reinforced by Figures 08, 09 and 10. Figure 08 highlights the northern and northeastern parts of the study area, which still maintain high vegetation cover and show minimal built-up development. As a result, these areas record relatively low land surface temperatures. Figure 09 illustrates the spatial patterns of vegetation index, built-up area index, and land surface temperature in the urban core of Galle, the most urbanized zone in the study area. The maps demonstrate that this area contains very limited vegetation or in some places, no vegetation at all paired with dense built-up structures, and consequently records high land surface temperatures. Additionally, Figure 10 identifies some of the most urbanized zones within the study area, such as Galle Fort, the Galle Harbor area, Karapitiya town, the expressway entrance, and the Kalehegana area. These locations display very limited green space and consistently high surface temperatures, further supporting the relationship between urban expansion, loss of vegetation, and increased land surface temperature.

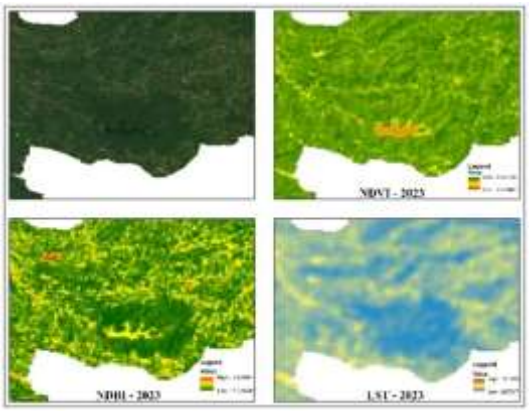

Fig.08: NDVI, NDBI and LST behavior in the northeastern part of the study area

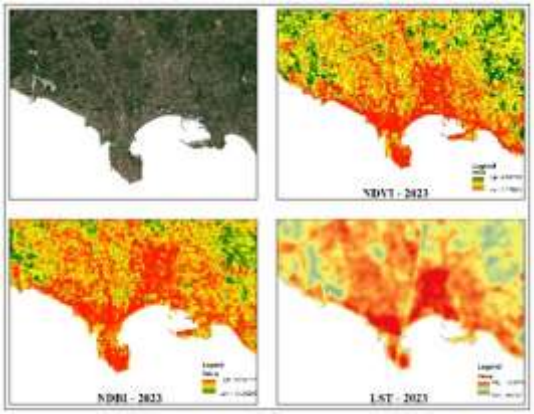

Fig.09: NDVI, NDBI and LST behavior in the Galle urban area

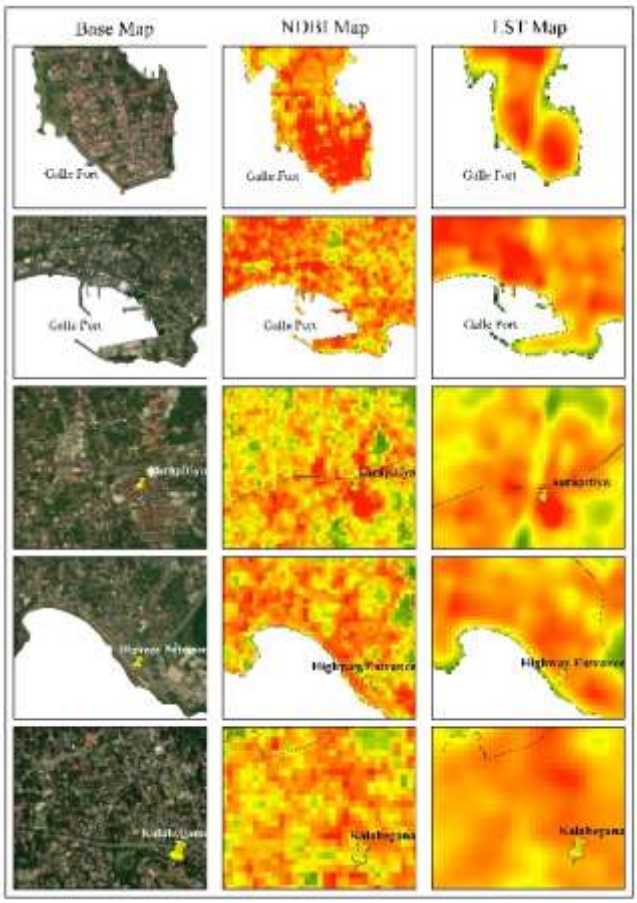

Fig.10: Normalized Difference Built-up Index and land surface temperature distribution in urbanized areas of the study area

Statistical Analysis of the Relationship between Land Surface Temperature, Vegetation Cover, and Built-Up Areas (2000–2024)

The relationship between the indicators NDVI, NDBI, and the land surface temperature (LST), which are used to analyze changes in green spaces in the Akmeemana, Bope-Poddala, and Galle Four Gravets Divisional Secretariat Divisions, was examined using the linear regression analysis method. To ensure statistical reliability and spatial representation, random point sampling was employed to extract sample values from each of the indicators.

Correlation Analysis between NDVI and NDBI in the Study Area

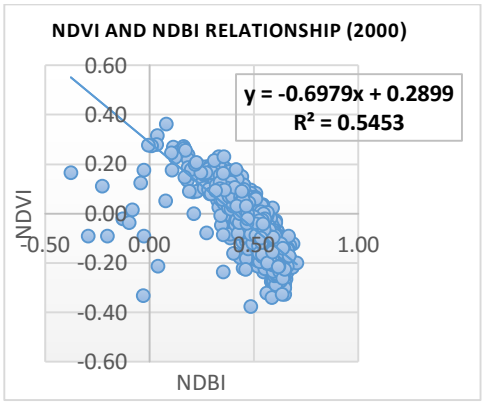

Fig.11: Relationship between NDVI and NDBI, 2000

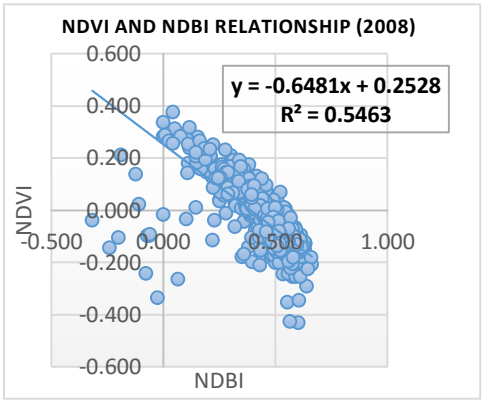

Fig.11: Relationship between NDVI and NDBI, 2008

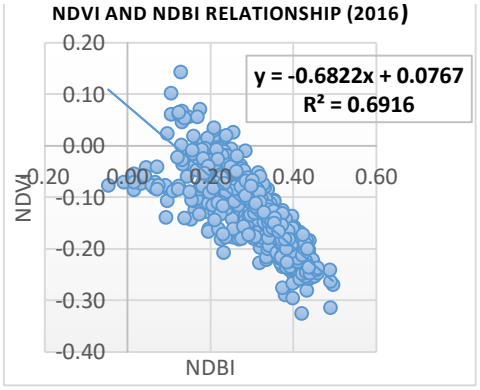

Fig.13: Relationship between NDVI and NDBI, 2016

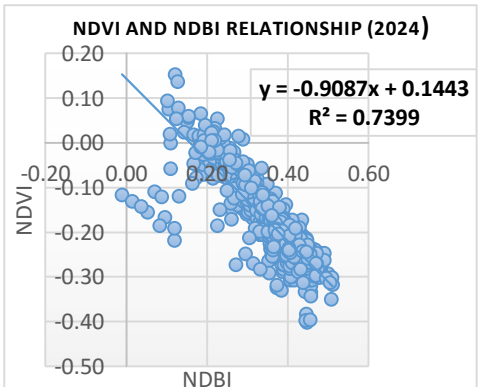

Fig.14: Relationship between NDVI and NDBI, 2024

A consistent negative correlation between NDBI and NDVI was observed throughout the study years 2000, 2008, 2016, and 2024, indicating that increases in built-up areas are associated with decreases in vegetation cover. In 2000, the slope coefficient of -0.6979 and correlation of -0.7384 revealed a strong inverse relationship, with 54.53% of NDVI variation explained by NDBI. A similar pattern was observed in 2008, with a slope of -0.6481, a correlation of -0.7391, and 54.63% explanatory power. In 2016, the relationship strengthened significantly (correlation = -0.8316), with 69.16% of NDVI variation explained by NDBI. The strongest correlation occurred in 2024 (correlation = -0.86), with a coefficient of determination of 0.7399, meaning 73.99% of the variation in vegetation cover was due to changes in built-up area. These findings confirm that as urbanization and built-up expansion increased, green spaces in the study area have significantly declined over time.

Correlation Analysis between NDVI and LST in the Study Area

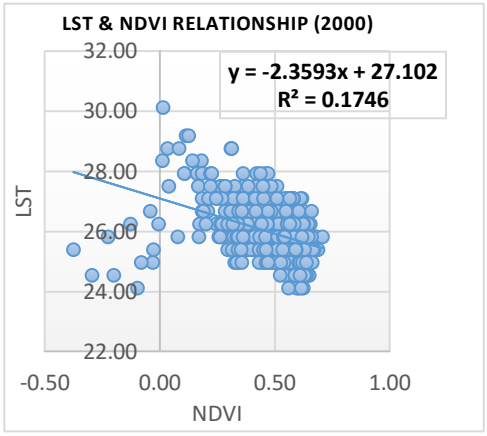

Fig.15: Relationship between NDVI and LST 2000

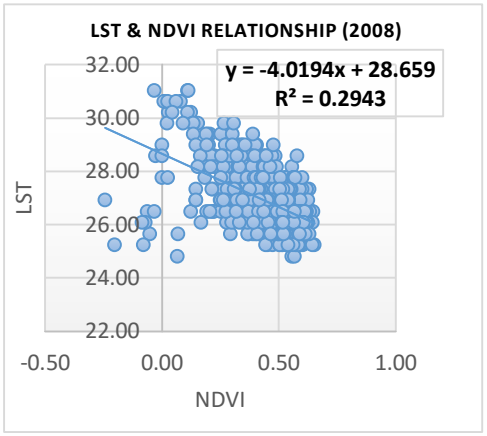

Fig.16: Relationship between NDVI and LST 2008

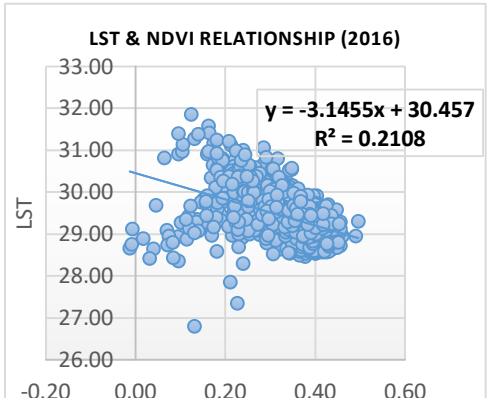

Fig.17: Relationship between NDVI and LST 2016

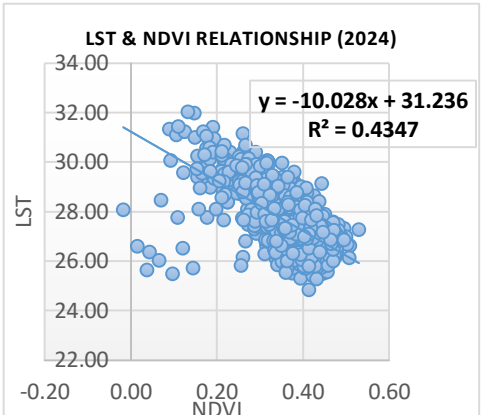

Fig.18: Relationship between NDVI and LST 2024

Throughout the years 2000, 2008, 2016, and 2024, a consistent negative correlation was observed between the Normalized Difference Vegetation Index (NDVI) and Land Surface Temperature (LST), indicating that areas with more vegetation tend to have lower surface temperatures. In 2000, a moderate negative correlation of -0.4178 was observed, with NDVI explaining 17.46% of the variation in LST, suggesting that vegetation had a limited influence on surface temperature due to the presence of other contributing factors. In 2008, the relationship strengthened (correlation = -0.5424), with NDVI accounting for 29.43% of LST variation, indicating a greater impact of vegetation on temperature regulation. By 2016, the correlation slightly weakened to -0.4591, with NDVI explaining 21.08% of the variability, showing continued influence of vegetation along with other factors. In 2024, the relationship became significantly stronger, with a correlation of -0.6593 and NDVI accounting for 43.47% of the LST variation, demonstrating a clearer link between vegetation loss and increased surface temperatures. These findings confirm that the reduction in green spaces has increasingly contributed to rising land surface temperatures in the study area over time

Correlation Analysis between NDBI and LST in the Study Area

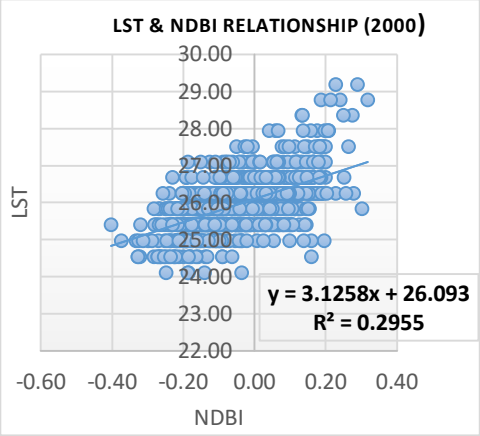

Fig.19: Relationship between NDBI and LST 2000

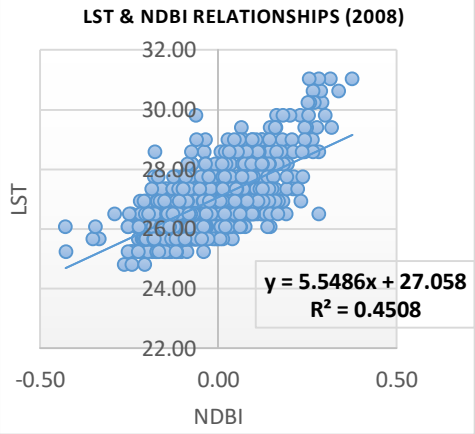

Fig.20: Relationship between NDBI and LST 2008

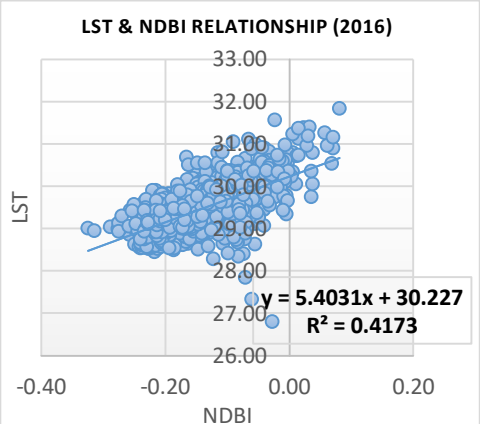

Fig.21: Relationship between NDBI and LST 2016

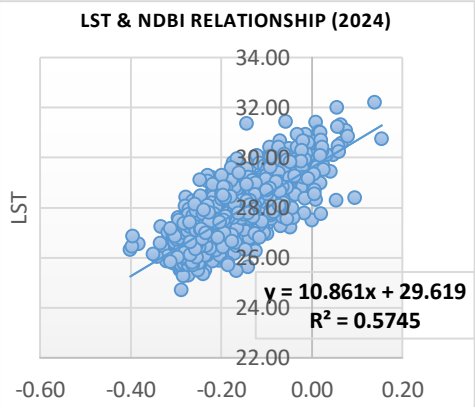

Fig.22: Relationship between NDBI and LST 2024

Between 2000 and 2024, a consistently positive correlation is observed between the Normalized Difference Built-up Index (NDBI) and Land Surface Temperature (LST), indicating that as built-up areas increase, surface temperatures rise accordingly. In 2000, the correlation is moderate (r = 0.5435), with NDBI explaining 29.55% of LST variability. This relationship strengthens in 2008 (r = 0.6714), where built-up areas account for 45.08% of LST changes, and remains strong in 2016 (r = 0.6459), explaining 41.73% of the variation. The strongest correlation is recorded in 2024 (r = 0.7579), with NDBI accounting for 57.45% of the variability in LST. The slope coefficients also increase across the years, showing that the temperature rise associated with built-up expansion becomes more intense over time.

These findings clearly confirm that the increase in built-up areas has led to a significant rise in land surface temperatures. Furthermore, this trend is closely tied to the simultaneous reduction of green spaces (as shown by the inverse correlation between NDVI and NDBI), indicating that urban expansion not only reduces vegetation cover but also contributes to urban heat through decreased natural cooling, and thereby intensifying surface temperatures.

5. Conclusion

This study examined the relationship between changes in green space and land surface temperature (LST) in the Akmeemana, Bope-Poddala, and Galle Four Gravets Divisional Secretariat Divisions from 2000 to 2024, focusing on how urbanization and the expansion of built-up areas have influenced local climatic conditions. The analysis utilized remote sensing, GIS, and statistical methods to assess variations in the Normalized Difference Vegetation Index (NDVI), Normalized Difference Built-up Index (NDBI), and LST across the study period.

The results clearly show a significant spatial and temporal increase in highly and very highly built-up areas, from 10.65 km² in 2000 to 28.84 km² in 2024, primarily due to rapid urban development, population growth, and large-scale infrastructure projects such as the Southern Expressway. Concurrently, a marked decrease in high and very high vegetation cover was observed, dropping from 94.49 km² in 2000 to 70.99 km² in 2024. This confirms that green spaces have been increasingly replaced by built-up areas over the past two decades.

Moreover, the study recorded a consistent rise in land surface temperature during the same period. The average LST increased by 1.63°C, while both the minimum and maximum LST values also showed upward trends. Spatial analysis reveals that temperature increases were most pronounced in areas where vegetation had decreased and built-up areas had expanded.

The statistical findings further reinforce these observations. A strong negative correlation was found between NDVI and NDBI (from -0.7384 in 2000 to -0.8601 in 2024), indicating that as urban areas grew, vegetation diminished. Similarly, a negative correlation between NDVI and LST (strengthening from -0.4178 to -0.6593) confirms that loss of green cover is directly associated with rising LST. Conversely, the positive correlation between NDBI and LST (increasing from 0.5435 to 0.7579) highlights that built-up expansion significantly contributes to temperature increases.

In conclusion, the study verifies that the increase in built-up areas has not only contributed to a reduction in green space but has also led to a consistent rise in land surface temperature in the study area. These findings emphasize the critical role of green infrastructure in regulating urban temperatures and underline the urgent need for sustainable urban planning and landscape management to balance development with environmental conservation**.**

6. References

1. *2016.pdf*. (n.d.). Retrieved June 6, 2025, from https://www.cs.sp.gov.lk/stat/2016.pdf.
2. *1686217885054609.pdf*. (n.d.). Retrieved June 8, 2025, from https://parliament.lk/uploads/documents/paperspresented/1686217885054609.pdf.
3. *CPH_2012_5Per_Rpt.pdf*. (n.d.). Retrieved June 5, 2025, from https://www.statistics.gov.lk/Resource/en/Population/CPH_2011/CPH_2012_5Per_Rpt.pdf.
4. Deforestation. (2025). In *Wikipedia*. https://en.wikipedia.org/w/index.php?title=Deforestation&oldid=1293988840#cite_note-4.
5. Dissanayake, D. (2020). Land Use Change and Its Impacts on Land Surface Temperature in Galle City, Sri Lanka. *Climate*, *8*(5), 65. https://doi.org/10.3390/cli8050065.
6. *Earth's Changing Climate*. (n.d.). Retrieved June 8, 2025, from https://education.nationalgeographic.org/resource/earths-changing-climate.
7. Estoque, R. C., Murayama, Y., & Myint, S. W. (2017). Effects of landscape composition and pattern on land surface temperature: An urban heat island study in the megacities of Southeast Asia. *The Science of the Total Environment*, *577*, 349–359. https://doi.org/10.1016/j.scitotenv.2016.10.195.
8. *Forests*. (n.d.). Retrieved June 5, 2025, from https://www.wwfnepal.org/forests.
9. Halefom, A., He, Y., Nemoto, T., Feng, L., Li, R., Raghavan, V., Jing, G., Song, X., & Duan, Z. (2024). The Impact of Urbanization-Induced Land Use Change on Land Surface Temperature. *Remote Sensing*, *16*(23), 4502. https://doi.org/10.3390/rs16234502.
10. *Land Surface Temperature*. (n.d.). Retrieved June 8, 2025, from https://earthobservatory.nasa.gov/global-maps/MOD_LSTD_M.
11. *Landsat Normalized Difference Vegetation Index | U.S. Geological Survey*. (n.d.). Retrieved June 8, 2025, from https://www.usgs.gov/landsat-missions/landsat-normalized-difference-vegetation-index.

12. Meegahakotuwa, U., & Nianthi, R. (2023). *Spatial and Temporal Variation of Temperature Trends in Last Century of Sri Lanka—2nd International Research Symposium—IRSUWC, February 1-2, 2018, Uva Wellassa University, Sri Lanka.*
13. Meyer, W. B., & Turner, B. L. (1992). Human Population Growth and Global Land-Use/Cover Change. *Annual Review of Ecology and Systematics*, *23*(1), 39–61. https://doi.org/10.1146/annurev.es.23.110192.000351.
14. Nations, U. (n.d.). *68% of the world population projected to live in urban areas by 2050, says UN*. United Nations; United Nations. Retrieved June 5, 2025, from https://www.un.org/uk/desa/68-world-population-projected-live-urban-areas-2050-says-un.
15. *NDBI—ArcGIS Pro | Documentation*. (n.d.). Retrieved June 8, 2025, from https://pro.arcgis.com/en/pro-app/latest/arcpy/spatial-analyst/ndbi.htm.
16. *Overview*. (n.d.). Retrieved June 8, 2025, from http://www.galle.dist.gov.lk/index.php/en/about-us/overview.html.
17. *Remote Sensing | NASA Earthdata*. (n.d.). Retrieved June 5, 2025, from https://www.earthdata.nasa.gov/learn/earth-observation-data-basics/remote-sensing?utm_source=chatgpt.com.
18. Rendana, M., Razi Idris, W. M., Abdul Rahim, S., Ghassan Abdo, H., Almohamad, H., Abdullah Al Dughairi, A., & Albanai, J. A. (2023). Effects of the built-up index and land surface temperature on the mangrove area change along the southern Sumatra coast. *Forest Science and Technology*, *19*(3), 179–189. https://doi.org/10.1080/21580103.2023.2220576.
19. Rocha, J., Oliveira, S., Viana, C. M., & Ribeiro, A. I. (2022). Climate change and its impacts on health, environment and economy. In *One Health* (pp. 253–279). Elsevier. https://doi.org/10.1016/B978-0-12-822794-7.00009-5.
20. *RS Ch 4 RS Preprocessing.pdf*. (n.d.). Retrieved June 8, 2025, from https://www.geo-informatie.nl/courses/grs10306/Clevers/RS%20CH4%20Preprocessing/RS%20Ch%204%20RS%20Preprocessing.pdf.
21. *State of the World's Forests 2020*. (n.d.). Retrieved June 5, 2025, from https://www.fao.org/state-of-forests/en/.
22. *Study Session 5 Urbanisation: Trends, Causes and Effects: View as single page | OLCreate*. (n.d.). Retrieved June 5, 2025, from https://www.open.edu/openlearncreate/mod/oucontent/view.php?id=79940&printable=1.
23. *What Is Normalized Difference Vegetation Index (NDVI)?* (2025, May 8). https://eos.com/blog/normalized-difference-vegetation-index-or-ndvi/.
24. *World of Change: Global Temperatures*. (2020, January 29). [Text.Article]. NASA Earth Observatory. https://earthobservatory.nasa.gov/world-of-change/global-temperatures?utm_source=chatgpt.com.
25. Zha, Y., Gao, J., & Ni, S. (2003). Use of normalized difference built-up index in automatically mapping urban areas from TM imagery. *International Journal of Remote Sensing*, *24*(3), 583–594. https://doi.org/10.1080/01431160304987.
26. *ශ්‍රී ලංකාවේ වන විනාශය – Environment Foundation (Guarantee) Limited.* (n.d.). Retrieved June 5, 2025, from https://efl.lk/loss_of_forest_cover_in_sl_sinhala/.

INFO

Corresponding Author: K.W.K.A Priyadarshana, Department of Geography and Environmental Management, Sabaragamuwa University of Sri Lanka, Belihuloya, 70140.

How to cite/reference this article: K.W.K.A Priyadarshana, H.M.K.C.W Herath, ANALYZING THE RELATIONSHIP BETWEEN LAND SURFACE TEMPERATURE AND THE SPATIAL PATTERN OF GREEN SPACE IN AKMEEMANA, BOPE-PODDALA AND GALLE FOUR GRAVETS DIVISIONAL SECRETARIAT DIVISIONS, *Asian. Jour. Social. Scie. Mgmt. Tech*. 2025; 7(4): 155-174.